Singlet oxygen generation by photodynamic agents

Jim M. Fernandez, Mehmet D. Bilgin, Leonard I. Grossweiner *

Wenske Laser Center, Ravenswood Hospital Medical Center, 4550 N. Winchester Ave., Chicago, IL 60640 USA

Abstract

The singlet oxygen quantum yield of photodynamic agents was measured at 546 nm, 630 nm, and on the far-red absorption peak. The technique employed is available in most laboratories, in which the photosensitization of lysozyme is used as an internal actinometer. Measurements in a pH 7.4 phosphate buffer plus 1% Triton X-100 (PB/X100) are scaled to 0.52 for methylene blue in the phosphate buffer. The average quantum yields are: hematoporphyrin IX (0.73), protoporphyrin IX (0.56) zinc protoporphyrin IX (0.91), mesotetra-(4-sulfonato–phenyl)porphine (0.61), Photofrin[R] (0.89), benzoporphyrin derivative monoacid ring-A (0.84), chlorin e6 in PB (0.64), pheophorbide a (0.69), and aluminum phthalocyanine tetrasulfonate (0.38). Protection factors were measured for added azide ion, 1,4-diazabicyclo[2.2.2]-octane, and superoxide dismutase. Spectral evidence is presented for chlorin e6 interactions with PB/TX100 and for binding to lysozyme.

1. Introduction

The energy efficiency of a Type II photosensitized process (photodynamic action) is limited by the singlet oxygen quantum yield (Φ_Δ). Many different techniques have been employed for measurements of Φ_Δ, including the "monomol"luminescence of singlet oxygen ($^1\Delta_g$) at 1270 nm, photothermal methods, EPR measurements of nitroxide radicals, oxygen uptake for a sensitized photo–oxidation, and quantum yields of the photochemical products. To be used in aqueous solution, hydrophobic sensitizers require solubilizing media that may affect the reactivity of $^1\Delta_g$ with an external probe. Measurements on self-aggregating sensitizers may depend on the concentration and wavelength owing to different Φ_Δ and extinction coefficients of the monomer and higher aggregates. The object of this study was to measure Φ_Δ for some photodynamic agents and photodynamic therapy (PDT) sensitizers at visible wavelengths. The photosensitized inactivation of hen lysozyme (LYS) was used as the probe for $^1\Delta_g$. Previous measurements on Photofrin[R] (PF) and hypericin (HY) [1–3] show that this technique is sensitive and reproducible, requiring only a light source, a wavelength selection device, and a spectrophotometer. The enzyme inactivation quantum yields are scaled to Φ_Δ of methylene blue (MB) in pH 7.4 phosphate buffer (PB) and com-

pared with the available literature. The involvement of $^1\Delta_g$ and superoxide (O_2^-) were tested by adding azide, 1,4 – diazabicyclo[2.2.2]-octane (DABCO), and superoxide dismutase (SOD).

2. Materials and methods

2.1. Chemicals

Hematoporphyrin IX (HF), methylene blue chloride (MB), protoporphyrin IX (PPIX), chicken egg white lysozyme, lyophilized *Micrococcus luteus*, bovine erythrocyte superoxide dismutase, sodium azide, 1,4-diazabicyclo[2.2.2]octane, Triton X-100, sodium laurel sulfate (SDS), and hexadecyltrimethylammonium bromide (CTAB) were obtained from Sigma Chemical Company; zinc protoporphyrin IX (ZnPP), chlorin e6 (Chl-e6), pheophorbide a (pheo-a), aluminum phthalocyanine tetrasulfonate (AlPcS$_4$), and mesotetra-(4-sulfonato-phenyl)porphine (TPPS) were obtained from Porphyrin Products, Inc. (Logan, UT); Photofrin[R] (PF) and benzoporphyrin derivative monoacid ring-A (BPD-MA) were obtained from QLT Phototherapeutics Inc. (Vancouver, BC). The chemicals were used as received. Optical absorption spectra were measured with a Perkin-Elmer Lambda 5 spectrophotometer. Fluorescence spectra were measured with a Farrand manual

* Corresponding author.

spectrofluorimeter. The MB concentration in PB was based on the 665 nm extinction coefficient of 78 000 M^{-1} cm^{-1} [4]. The other sensitizer concentrations were calculated by stoichiometry. An Ophir Model D6X Laser Power/Energy meter was used to measure the incident irradiance.

2.2. Assay of lysozyme activity

LYS activity was assayed by the lysis rate of lyophilized *M. luteus*. The light-scattering optical density of the substrate (OD_{sc}) was measured at 700 nm after 100-fold dilution in a pH 6.24, 10 mM phosphate buffer. The sensitizer absorption was negligible under the assay conditions. The prior work shows that a semilogarithmic plot of OD_{sc} vs the assay time (t') has a constant initial slope followed by leveling at long t' [1–3]. The enzymic activity rate constant (β) was calculated by non-linear least-squares fitting to the semi-empirical rate equation.

$$OD_{sc} = OD_o[1 + b \exp(-\beta t')] \tag{1}$$

where b is constant for irradiated and unirradiated solutions.

2.3. Irradiations

Measurements were made in 10 mM, pH 7.4 phosphate buffer plus 1% Triton X-100 (PB/TX100) unless otherwise indicated. The light source was a 200 W high-pressure Hg–Xe arc (Oriel model 6291) filtered by a Corning C.S. No. 0-52 glass filter (> 360 nm) and 2 cm of water. A Bausch & Lomb "high intensity" grating monochromator was used for wavelength selection with 5 mm entrance and exit slits (30 nm dispersion). The measurements at 546 nm were performed with a narrow-band interference filter (9 nm full-width at half-height). The 5 ml samples were contained in a cylindrical glass cuvette (diameter, 2 cm; length, 2 cm) located in a temperature-controlled holder at 25.0 °C with stirring by a small magnetic bar and slow bubbling with oxygen. The incident beam diameter was 6 mm at the front face of the irradiation cuvette. Activity assays were performed at 5 min intervals for 35 min. The LYS concentration in all runs was either 15 or 30 μM. Semi-logarithmic plots of β vs the irradiation time (t) had a constant initial slope, followed in some cases by leveling attributed to sensitizer photobleaching. A similar functional form as Eq. (1) was used to calculate the initial photoactivation rate constant (Γ)

$$\beta(t) = \beta_d[1 + C_1 \exp(-\Gamma t)] \tag{2}$$

where β_d is the dark activity constant and C_1 is a constant. The procedure is equivalent to extrapolating the semilogarithmic plot to zero time. The values of Γ (min^{-1}) for a given sensitizer vary with wavelength owing to changes in the incident power and sensitizer absorption.

2.4. Calculation of quantum yields

The photosensitized inactivation of an aqueous enzyme via a Type II, $^1\Delta_g$ mechanism obeys the following dose-response relation

$$-\log_e(L/L_o) = \Phi_c E_{abs}/L_o \tag{3}$$

where Φ_c is the enzyme inactivation quantum yield, L_o (M) is the total enzyme concentration, L (M) is the active enzyme concentration, and E_{abs} is the absorbed light dose in moles of photons or "einsteins" per liter [5]. The derivation of Eq. (3) assumes that the total rate of $^1\Delta_g$ reactions with the enzyme is not affected by inactivation. Differentiation of Eq. (3) with respect to E_{abs} confirms Φ_c is the initial photoinactivation quantum yield. The calculation of Φ_c from the experimental values of Γ is based on

$$\Phi_c = 1.9938 \frac{\Gamma(\min^{-1}) V(cm^3) L_o(\mu M)}{P_o(mW) f_{abs} \lambda(nm)} \tag{4}$$

where Γ is first-order photoinactivation rate constant in Eq. (2), V is the constant irradiated volume (5.0 ml), P_o is the incident power at the irradiation wavelength λ, and f_{abs} is the fractional absorption by the sensitizer. Values of P_o were calculated at each λ from parallel measurements on MB, as described below. The following expression was used to calculate f_{abs}

$$f_{abs} = (1 - R)[1 - 10^{-OD'd}] \tag{5}$$

where OD' is the optical density per cm of the sensitizer as measured in the spectrophotometer at the irradiation wavelength, d is the optical path of the irradiation cuvette, and R is the specular reflection coefficient at the air-glass-water interface of the irradiation cuvette, which was taken as 0.03 for visible light. Φ_Δ was calculated from Φ_c with the steady-state kinetics relation

$$\Phi_\Delta = \Phi_c[(1/\tau_\Delta) + kL_o]/k'L_o \tag{6}$$

where k is the total bimolecular rate constant for $^1\Delta_g$ reactions with LYS, k' is the corresponding bimolecular rate constant for inactivation, and τ_Δ is the solvent-induced decay lifetime of $^1\Delta_g$. Literature values of the rate constants calculated from photosensitization of LYS by acridine orange are $k = 4.4 \times 10^8$ M^{-1} s^{-1} and $k' = 2.9 \times 10^7$ M^{-1} s^{-1} [6]; τ_Δ was taken as 3.9 μs in PB [7]. The dependence of Φ_Δ on the numerical values of k, k' and τ_Δ was minimized or eliminated by scaling the measurements to a standard photosensitizer. For measurements at the same P_o and λ, Eqs. (4)0 and (6) lead to

$$\Phi_\Delta / \Phi_\Delta^* \frac{[1/\tau_\Delta + kL_o]}{[1/\tau_\Delta + kL_o^*]} (f_{abs}^*/f_{abs})(\Gamma/\Gamma^*) \tag{7}$$

where * refers to the standard. Thus for a given Φ_Δ^*, Φ_Δ does not depend on k' for any L_o and is independent of $k\tau_\Delta$ when the sensitizer and standard are measured at the same L_o. Otherwise, there is a small dependence of the calculated

Φ_Δ on $k\tau_\Delta$, e.g., a two-fold change in $k\tau_\Delta$ leads to a 1%–2% change in the calculated Φ_Δ when the sensitizer is measured at $L_o = 30$ μM and the standard is measured at $L_o^* = 15$ μM.

The present scaling is based on the absolute measurement of $\Phi_\Delta = 0.52$ for aqueous MB [8]. The measurements at each irradiation wavelength were paralleled by measurements of Φ_c for MB in PB. Substituting the experimental Φ_c for MB and $\Phi_\Delta = 0.52$ in Eqs. (4) and (6) gives the effective P_o for measurements at that wavelength. With this procedure P_o is a scaling factor. The calculated P_o should be comparable to the incident power as measured with a conventional radiometer, although the two values may not be the same owing to the spectral bandwidth of the light source and beam deviations from ideal collimation. Some comparisons are: 546 nm interference filter: (38 mW, 34 mW); monochromator: 630 nm (34 mW, 34 mW), 644 nm (26 mW, 26 mW), 660 nm (24 mW, 21 mW), 668 nm (16 mW, 14 mW), where the first value is P_o calculated from the MB actinometer and the second value was measured with the Ophir power meter.

2.5. Effects of additives

The effects of additives on Φ_c were evaluated by the protection factor (p)

$$p = (\beta_p - \beta_o) / (\beta_d - \beta_o) \tag{8}$$

where β_p, β_o, and β_d are the enzymic activity constants for irradiations with the additive, irradiations without the additive, and in the dark, respectively [1–3]. p ranges from 0 for no protection to 1 for complete protection. The value of p depends on the activity loss induced by the light and the type and concentration of the protective agent, e.g., $p = 0.5$ for an irradiation that halves the dark activity in the absence of the additive and reduces the activity 25% in the presence of the additive.

3. Results

3.1. Photosensitization of lysozyme

Table 1 summarizes the photoinactivation results. The measurements at 546 nm were made with the interference filter and measurements at other wavelengths were made with the monochromator. The good agreement indicates that the larger bandwidth of the monochromator was not a significant source of error. The sensitizer and MB were measured at the same L_o except as noted by an asterisk. The values of Φ_Δ are not different for this group. The prior hypericin measurement was made with 30 μg ml^{-1} SOD to suppress the contribution of O_2^- [2]. Except for PF at 630 nm, Φ_c and Φ_Δ are independent of wavelength within the experimental variations. The high Φ_Δ for PF at 630 nm was found also in the prior work and attributed to a photosensitizing photoproduct [1] (see Discussion).

Chl–e6 had a very low Φ_Δ in PB/TX100. Increasing the TX100 concentration to 3% did not lead to significant values of Γ. The absorption and fluorescence shifts in PB and PB/TX100 are indicative of a dark interaction between Chl–e6 and TX100 (Table 2). Similar fluorescence results were reported in a recent study on Chl–e6 and N-aspartyl chlorine6 (NPe6) [9]. There is ample evidence that serum albumin and many other proteins strongly bind Chl–e6 [10]. Binding of Chl–e6 to LYS in PB and PB/TX100 is indicated by the spectral shifts in Table 2. The negligible photosensitization of LYS by Chl–e6 in PB/TX100 may be a consequence of this interaction. Weak photosensitization was found in 3% SDS and 6% SDS and Φ_Δ was approximately the same in PB and 3% CTAB (Table 1). The solvent effects indicate that specific reactions of Chl–e6 with the detergent micelles are involved.

BPD-MA is aggregated in PBS-methanol mixtures containing less than 30% methanol [11]. The effects of the BPD-MA concentration and the medium on Φ_Δ are summarized in Table 3. At 1.1 μM BPD-MA, Φ_Δ increases from 0.64 in PB to 0.86 in PB/3%TX100; at 16 μM BPD-MA, Φ_Δ increases from 0.17 in PB to 0.35 in PB/3%TX100. The average $\Phi_\Delta = 0.78$ for 6 μM BPD-MA in PB/TX100 (Table 1) falls between these values. The results in Table 3 can be explained by the monomer-dimer equilibrium for BPD-MA (see Discussion). The values of Φ_Δ in PB/1%TX100 and PB/3%TX100 for 1.1 μM BPD-MA are statistically the same. The mean 0.84 ± 0.03 is taken as the best value.

3.2. Effect of additives

The protection factors are summarized in Table 4. The average values of p for 4 min irradiations at 630 nm are 0.40 ± 0.13 for 10 mM azide and 0.41 ± 0.09 for 2 mM DABCO, excluding PF and Chl–e6. Some variations in the individual values are expected owing to the dependence of p on the effect of the light. Significant protection by azide and DABCO indicate the involvement of $^1\Delta_g$ for all sensitizers except Chl–e6 in PB. The low values of p with added SOD may not rule out a small yield of O_2^- if $^1\Delta_g$ accounts for most of the inactivation (see Discussion). According to steady-state competition kinetics, a plot of $1/\Phi_c$ vs the acceptor concentration should be linear with the slope:intercept ratio equal to: $k_p / [kL_o + 1/\tau_\Delta]$; k and k_p are the total bimolecular rate constants for $^1\Delta_g$ reactions with LYS and the acceptor, respectively. The effect of the azide concentration on Φ_c was measured at 630 nm for ZnPP in PB/TX100 and for MB in PB (Fig. 1). The MB measurements lead to $k_p = (9 \pm 5) \times 10^8$ M^{-1} s^{-1} in PB. This result is comparable to the literature values of k_p for azide quenching of $^1\Delta_g$ in water or buffer: 8×10^8 [6], 5×10^8 [12], 1.5×10^9 [13], 6×10^8 [14], and $(2–3) \times 10^8$ [15]. The generation of O_2^- by MB is ruled out by the results in Ref. 2. The measurement for ZnPP in PB/TX100 gives $k_p = (1.0 \pm 0.3) \times 10^7$ M^{-1} s^{-1}. A small contribution from O_2^- cannot be excluded. The straight lines in Fig. 1 provide additional evidence that azide

Table 1
Summary of Φ_e and Φ_Δ measurements

Sens. [a]	λ (nm)	[LYS] [b] (μM)	$10^3 \times \Phi_e$ [c]	Φ_Δ
9.1 μM MB/PB	630	15	0.860±0.044 (8)	(0.52)
9.1 μM MB/TX100	630	15	0.78±0.04 (4)	0.49±0.03
	546	15	0.82±0.08 (3)	0.49±0.04
				0.49±0.02
17 μM HP/TX100	630	15	1.21±0.07 (3)	0.74±0.04
	546	15	1.13±0.08 (3)	0.69±0.08
	500	15	1.23±0.06 (2)	0.75±0.03
				0.73±0.03
10 μM PPIX/TX100	646	15	0.99±0.06 (3)	0.60±0.05
	630	15	0.89±0.05 (3)	0.54±0.04
	546	15	0.89±0.04 (3)	0.54±0.03
				0.56±0.03
12 μM ZnPP/TX100	630	15	1.36±0.13 (3)	0.82±0.08
	546	15	1.28±0.09 (3)	0.91±0.12
	426	15	1.64±0.18 (3)	0.99±0.11
				0.91±0.09
8 μM TPPS/TX100	644	30	2.01±0.02 (3)	0.62±0.01
	630	30 *	1.87±0.02 (3)	0.58±0.01
	546	30	1.81×0.21 (3)	0.56±0.08
	424	30 *	2.22±0.05 (3)	0.69±0.02
				0.61±0.06
9 μM PF/TX100 [d]	630	30 *	4.50±0.06 (2)	>1 [e]
	546	30	2.96±0.30 (3)	0.91±0.12
	514	30	2.83±0.02 (2)	0.87±0.01
				0.89±0.03
12 μM Chl-e6/PB	660	30	2.44±0.16 (4)	0.75±0.05
	630	30 *	2.03±0.12 (3)	0.62±0.04
	546	30	1.82±0.04 (2)	0.56±0.01
				0.64±0.10
12 μM Chl-e6/1%TX100	660	30	0.15±0.01 (4)	0.05±0.01
	630	30 *	0.12±0.01 (3)	0.04±0.01
12 μM Chl-e6/3%TX100	660	30	0.1±0.1 (2)	0.00
12 μM Chl-e6/3%SDS	660	30	0.42±0.09 (2)	0.13±0.03
12 μM Chl-e6/3%CTAB	660	30	1.93±0.01 (2)	0.59±0.01
6 μM BPD-MA/TX100	692	30	2.55±0.22 (4)	0.79±0.09
	630	30 *	2.53±0.22 (8)	0.77±0.08
	546	30	1.34±0.14 (2)	0.76±0.10
				0.78±0.02
12 μM Pheo-a	668	15	1.17±0.05 (3)	0.71±0.04
	630	15	1.17±0.04 (3)	0.71±0.04
	546	15	1.09±0.05 (3)	0.66±0.04
				0.69±0.03
8 μM AlPcS$_4$/TX100	673	30	1.41±0.12 (4)	0.43±0.04
	630	30 *	1.28±0.11 (4)	0.39±0.03
	546	30	1.06±0.02 (2)	0.33±0.01
				0.38±0.05
7 μM HY/TX100 [f]	590	30	1.64±0.22 (16)	0.49±0.06

[a] 'TX100' refers to 10 μM, pH 7.4 phosphate buffer plus 1% Triton X-100 unless indicated otherwise.
[b] The scaling MB runs were performed at the same L_0 as the sensitizer except for runs indicated * at 15 μM LYS.
[c] Number of runs in parenthesis.
[d] Based on nominal 600 D molecular weight.
[e] See text.
[f] Pooled data for hypericin and sodium hypericin with 30 μg ml^{-1} SOD; from Ref. 2.

reacted with $^1\Delta_g$ in the external medium. The 100-fold lower rate compared to PB explains why relatively high azide concentrations are required to achieve significant protection. Literature values of k_p for DABCO in polar organic solvents are the order of 1×10^7 [16]. The comparable protection by 10 mM azide and 2 mM DABCO suggests that the reaction of $^1\Delta_g$ with DABCO in PB/TX100 was faster than with azide. Increasing the acceptor concentrations to 100 mM azide and 20 mM DABCO had no protective effect for Chl–e6 in PB. However, the inability of the acceptors to protect LYS does

Table 2
Effects of TX100 and LYS on Chl-e6 absorption and fluorescence spectra

Medium [a]	Absorption peak [b]	Fluorescence peak [c]
PB	651.5±0.1	667
PB+3 μM LYS	652.4±0.1	658
PB+10 μM LYS	656.2±0.0	654
PB+30 μM LYS	656.4±0.1	654
PB+100 μM LYS	656.4±0.0	654
TX100	661.1±0.1	674
TX100+3 μM LYS	662.0±0.2	670
TX100±10 μM LYS	662.3±0.0	668
TX100+30 μM LYS	662.3±0.1	668
TX100+100 μM LYS	662.4±0.1	665

[a] 12 μM Chl-e6 in 10 mM, pH 7.4 PB or PB/TX100.
[b] Average of four measurements.
[c] Average of three measurements; excited at 570 nm; uncorrected.

not rule out the generation of $^1\Delta_g$. Oxygen uptake experiments led to high values of Φ_Δ for Chl–e6 and other chlorins in PB [17].

4. Discussion

The present methodology is based on the assumption that the rate of LYS photoinactivation is proportional to the rate of $^1\Delta_g$ generation by the sensitizer. The reactivity of LYS towards $^1\Delta_g$ is shown by prior work with many sensitizers, including acridine orange [6], MB [18,19], eosin Y [5], 8-methoxypsoralen [20], proflavine [19], acriflavine [19], and HY [3]. Possible interfering factors are aggregation of the sensitizer and sensitizer binding to LYS. The sensitizers investigated in this work have a wide range of absorption properties. Aqueous MB absorbs at 665 nm. The typical free-base porphyrin absorption consists of the intense Soret band (B band) near 400 nm and four weak bands of decreasing intensity from 450–700 nm (Q bands). Metalloporphyrins have two Q bands of approximately equal intensity, e.g., near 540 and 580 nm for ZnPP. The dominant chlorin absorptions are the Soret band near 400 nm and a strong band in the region of 600–700 nm. Metal-free phthalocyanines have visible bands of increasing intensity from 500–700 nm. The far-red absorption band dominates in AlPcS$_4$. The dominant visible absorption of HY is an intense narrow band near

590 nm. In the present work, the constant Φ_Δ at different wavelengths and the generally good agreement with other measurements (Table 5) support the validity of the LYS actinometer methodology.

4.1. Singlet oxygen quantum yields

The experimental data required for measurements of Φ_Δ are the photoinactivation rate constants Γ for the sensitizer and MB at the same wavelength and OD'. The exact sensitizer concentrations and extinction coefficients are not required. The average values of Φ_Δ in Table 1 are compared with the available literature in Table 5.

4.1.1. Methylene blue

Measurements of Φ_Δ for MB in water, micelles, and alcohols are close to 0.52 used as the standard for MB in PB. The prior results were scaled to different standards, except Ref. 8 which was based on radiometry. The average of the prior work, 0.49±0.07 agrees with the present measurement in PB/TX100 of 0.49±0.02 [2,8,21–23]. The values of Φ_Δ are consistent with a recent determination of the MB triplet yield (Φ_T) in methanol which led to 0.50±0.02 [24]. The good agreement between P_o calculated with Φ_Δ = 0.52 for MB in PB and measurements with the power meter provides independent support for the present actinometry.

4.1.2. Porphyrins

Three measurements for HP in methanol based on different methods average to Φ_Δ = 0.65 ± 0.12. The dependence on the HP concentration in PB reported in prior work at 546 nm, based on the photo-oxidation of N,N.-dimethyl-4-nitrosoaniline (RNO), led to decreasing Φ_Δ from 0.45 at 3 μM to 0.36 at 150 μM [23]. The concentration effect is explained by new results on the equilibrium between the monomer and dimer, each of which has a different Φ_Δ and extinction coefficient [26]. The calculations indicate that the experimental Φ_Δ at 546 nm should decrease from 0.43–0.32 from 3–150 μM. The present Φ_Δ = 0.73 ± 0.03 in PB/TX100 agrees with 0.74 calculated for the HP monomer in pH 7.4 PB and 0.76 in methanol [26]. Several lower values of Φ_Δ for aqueous HP are reported in other work [23,27].

The present Φ_Δ = 0.56 ± 0.03 for PPIX in PB/TX100 agrees with Φ_Δ = 0.57 for protoporphyrin dimethylester in

Table 3
Effect of concentration and medium on photosensitization of LYS by BPD-MA [a]

BPD-MA Conc.	1.1 μM		16 μM	
Medium	Absorption peak (nm)	Φ_Δ	Absorption peak (nm)	Φ_Δ
PB	692	0.64±0.04 (3)	694	0.17±0.01 (2)
PB/1%TX100	689	0.82±0.07 (3)	689	0.32±0.01 (3)
PB/3%TX100	687	0.86±0.04 (3)	687	0.35±0.03 (3)

[a] Irradiated at 546 nm; number of runs in parenthesis.

Table 4
Effect of additives on photosensitization of LYS in PB/TX100

Additive:	Protection factor [a]		
Sens. [b]	SOD (30 mg ml^{-1})	Azide (10 mM)	DABCO (2 mM)
MB (9.1 μM)	0.00	0.24	0.31
HP (17 μM)	0.01	0.32	0.35
PPIX (10 μM)	0.03	0.55	0.48
ZnPP (12 μM)	0.02	0.39	0.38
TPPS (8 μM)	0.03	0.34	0.52
PF (9 μM)	0.03	0.19	0.38
Chl-e6 (6 μM) [c]	0.00	0.00 [d]	0.00 [d]
BPD-MA (6 μM)	0.04	0.56	0.51
Pheo-a (12 μM)	0.03	0.56	0.42
AlPcS$_4$ (8 μM)	0.02	0.39	0.31

[a] Ranges from 0 for no protection to 1 for complete protection.
[b] Measured at 630 nm in PB/TX100 unless indicated.
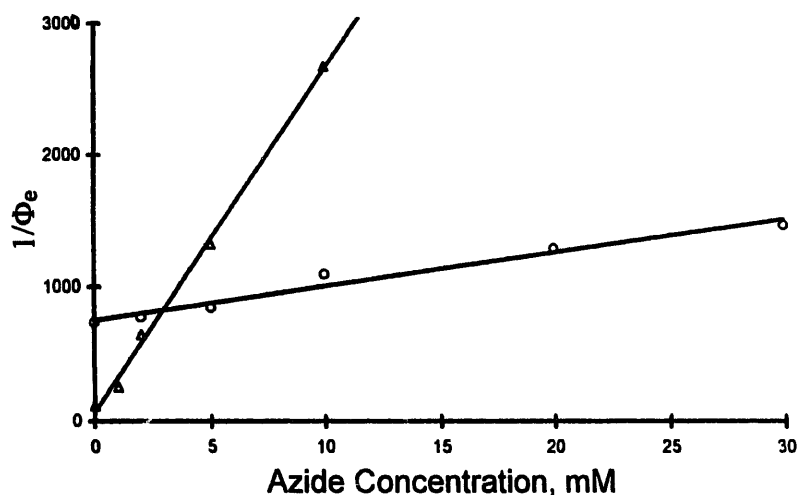[c] Measured in PB.
[d] 100 mM azide; 20 mM DABCO.

Fig. 1. Dependence of LYS inactivation quantum yield (Φ_e) on azide concentration: △ 9.1 μM methylene blue in 10 mM, pH 7.4 phosphate buffer (vertical axis divided by ten); ○ 12 μM zinc protoporphyrin in 10 mM, pH 7.4 phosphate buffer plus 1% Triton X-100.

benzene [28]. The present $\Phi_\Delta = 0.91 \pm 0.09$ for ZnPP in PB/TX100 is consistent with the very low fluorescence efficiency in polar (0.03) and non-polar (0.04) solvents and $\Phi_T \simeq 0.92$ [29]. $\Phi_\Delta = 0.88$ was reported for zinc meso-tetra(4-N-methylpyridyl) porphine in water [30].

The present $\Phi_\Delta = 0.61 \pm 0.06$ for TPPS in PB/TX100 is in excellent agreement with the average of literature values of 0.62 ± 0.01 [27,31,32].

The effect of the medium on Φ_Δ of the porphyrin mixture PF is discussed in Ref. 1. The present $\Phi_\Delta = 0.89 \pm 0.03$ in PB/TX100 (514,546 nm) agrees with 0.85 ± 0.11 at 514 nm measured with a tunable dye laser [1] and 0.87 ± 0.15 measured with the RNO method at 546 nm in egg phosphatidylcholine liposomes [23]. The apparent yield of 1.38 ± 0.14 nm measured at 630 nm with the arc lamp-monochromator agrees with the prior measurement of 1.27 ± 0.19 with the dye laser [1]. The latter result was attributed to the formation of a photosensitizing photoproduct with its far-red

absorption at 663 nm. This mechanism is supported by experiments in which PF in PB/TX100 was pre-irradiated at 630 nm. A subsequent irradiation at 650 nm led to a ten-fold increase of β compared with samples that were not pre-irradiated. The formation of the photoproduct was inhibited by azide and imidazole indicating that the photolysis reaction is mediated by $^1\Delta_g$. Chlorin-type photoproducts with similar far-red absorptions have been identified for PP, HP, and hematoporphyrin derivative and attributed to oxidation of a double bond by $^1\Delta_g$ [33].

4.1.3. Chlorins

Many chlorins are good photodynamic sensitizers in PB including mesochlorin, Chl-e6, NPe6 (also abbreviated as "MACE"), and di-L-aspartyl chlorin e6 (DACE) [17,32,34]. Oxygen uptake measurements for Chl-e6 in PB based on photo-oxidation of furfuryl alcohol led to $\Phi_\Delta = 0.66$ [17], which is in good agreement with the present 0.64 ± 0.10

Table 5
Summary of singlet oxygen quantum yields [a]

Sens.	Medium	Method	λ (nm)	Φ_Δ	Ref.
MB	H$_2$O	DMF oxidation	-	0.52 [b]	[8]
	methanol	1270 nm emission	430–750	0.58 [c]	[21]
	ethanol	DMA photo-oxidation	633	0.45 [d]	[22]
	pH 7.4 PB	RNO photo-oxidation	546	0.39 [e]	[23]
	PB/TX100	LYS photosens.	630	0.47 [f]	[2]
	PB/TX100	LYS photosens.	546, 630	0.49 [f]	this work
HP	methanol	1270 nm emission	430–750	0.53 [c]	[21]
	methanol	DPBF photo-oxidation	532	0.65	[25]
	methanol	O$_2$ uptake	535–576	0.76 [g]	[26]
	pH 7.4 PB	RNO photo-oxidation	546 (3 μM)	0.45 [e]	[23]
	pH 7.4 PB	O$_2$ uptake	Soret band	0.36 [c]	[27]
	SDS/D$_2$O	O$_2$ uptake	532	0.27	[25]
	CTAB/D$_2$O	O$_2$ uptake	532	0.22	[25]
	PB/TX100	LYS photosens.	500, 546, 630	0.73 [f]	this work
PPIX	PB/TX100	LYS photosens.	546, 630, 646	0.56 [e]	this work
ZnPP	PB/TX100	LYS photosens.	426, 546, 630	0.91 [f]	this work
TPPS	PB	O$_2$ uptake	424	0.62	[31]
	TX100	O$_2$ uptake	638	0.63	[32]
	pH 7.4 PB	O$_2$ uptake	Soret	0.61 [c]	[27]
	PB/TX100	LYS photosens.	424, 546, 630, 644	0.61 [f]	this work
PF	PB/TX100	LYS photosens.	514	0.85 [f]	[1]
	EPC liposomes	RNO photo-oxidation	546	0.87 [g]	[23]
	PB/TX100	LYS photosens.	514, 546	0.89 [f]	this work
Chl-e6	PB	O$_2$ uptake	654	0.66 [g]	[17]
	PB	LYS photosens.	546, 630, 660	0.64 [f]	this work
	PB/CTAB	LYS photosens.	660	0.59 [f]	this work
BPD-MA	benzene	1270 nm emission	335	0.77 [h]	[35]
	PB/TX100	LYS photosens.	546, 630, 692	0.84 [f]	this work[i]
Pheo-a	D$_2$O/TX100 + 10% ethanol	1270 nm emission	337	0.70 [i]	[36]
	PB/TX100	LYS photosens	546, 630, 668	0.69 [f]	this work
ALPcS$_2$	pH 7.2 Tris	O$_2$ uptake	424, 666	0.225 [j]	[37]
AlPcS$_3$	D$_2$O	1270 nm ᵓmission	355	0.34 [k]	[38]
'AlPcS'	pH 7.0 PB	RNO photo-oxidation	440	0.34 [c]	[39]
AlPcS$_4$	PB/TX100	LYS photosens.	546, 630, 673	0.38 [f]	this work
HY	BRIJ35	DPIB photo-oxidation	308	0.72	[40]
	PB/TX100/SOD	LYS photosens.	514, 575, 580, 585, 590, 600	0.49 [e]	[2]

[a] Abbreviations: DMF, 2,5-dimethylfuran; DMA, 9,10-dimethylanthracene; DPIB, 1,3-diphenylisobenzofuran; RB, rose bengal, CTAB, cetyltrimethyl-ammonium bromide; RNO, p-nitrosodimethylaniline.
[b] Absolute measurement.
[c] Scaled to Φ_Δ = 0.53 for HP in ethanol.
[d] Based on steady-state kinetics.
[e] Scaled to Φ_Δ = 0.75 for aqueous RB.
[f] Scaled to Φ_Δ = 0.52 for MB in water.
[g] Scaled to Φ_Δ = 0.79 for aqueous RB.
[h] Scaled to Φ_Δ = 1.0 for fullerene C$_{60}$.
[i] Scaled to 0.70 for TPPS.
[j] Scaled to 0.62 for TPPS.
[k] Scaled to 0.67 for TPPS.
[l] From Table 3.

in PB. The spectral data in Table 2 indicate significant binding of Chl–e6 to LYS in PB, which apparently does not affect Φ_Δ. However, protection by high azide and DABCO were totally ineffective. These water-soluble agents may not inhibit the transfer of $^1\Delta_g$ from the dye binding site to the enzyme inactivation site. The spectral results in Table 2 suggest that the negligible photosensitization of LYS by Chl–e6 in 1%–3% TX100 involves a specific interaction in uncharged

micelles. The weak sensitization for anionic SDS and strong sensitization for cationic CTAB indicate that the micellar charge is an important factor.

The present Φ_Δ = 0.84 ± 0.03 for BPD-MA in PB/TX100 is in good agreement with recent values of 0.78 and 0.80 in benzene and 0.76 in methanol [35]. Measurements on BPD-MA in aqueous micelles led Φ_T = 0.75 in TX100, SDS, and CTAB [11]. The results in Table 3 are explained by consid-

ering the monomer-dimer equilibrium. The dimerization constant of 9×10^6 M^{-1} was determined for aqueous BPD-MA [11]. The calculated monomer fraction in PB is 0.33 at 1.1 μM and 0.11 at 16 μM. Comparing with the Φ_Δ measurements, (Table 3) shows that $^1\Delta_g$ generation was about four times higher at the lower concentration, which is comparable with the calculated ratio for the monomer fractions. Exact agreement requires only a 3% contribution to $^1\Delta_g$ from the BPD-MA dimer at 546 nm. This case parallels aqueous HP in which a significant yield of $^1\Delta_g$ is generated by a partially aggregated sensitizer owing to the dominance of the monomer Φ_Δ.

The present $\Phi_\Delta = 0.69 \pm 0.04$ for Pheo-a in PB/TX100 agrees 0.70 in D$_2$O/2% TX100/10% ethanol [36].

4.1.4. Tetrasulfonated aluminum phthalocyanine

Results reported for sulfonated aluminum phthalocyanine are given in Table 5 [37–39]. The present measurements for AlPcS$_4$ in PB/TX100 give $\Phi_\Delta = 0.38 \pm 0.05$. The available data indicate that the extent of sulfonation has a small effect on Φ_Δ.

4.1.5. Hypericin

Free base hypericin (HY) and the sodium salt (HY–Na) are insoluble in water. Prior Φ_Δ measurements were reported for each starting material in PB/0.5% TX100 for monochromatic irradiations with a tunable dye laser at 590 nm. The equilibrium ionic state of HY after solubilization is unknown. The pooled average of the measurements led to $\Phi_\Delta = 0.49 \pm 0.06$ for HY with SOD and 0.58 ± 0.08 without SOD [2]. A measurement on HY in BRIJ 35 led to 0.72 ± 0.03 based on photo-oxidation of 1,3-diphenylisobenzofuran [40]. The poor agreement between the two measurements has not been explained.

4.2. Generation of superoxide

Electron transfer from the sensitizer triplet state to molecular oxygen is the usual pathway of O$_2^-$ formation in oxygenated aqueous solutions [41]. This process competes with physical quenching of the triplet state and energy transfer leading to $^1\Delta_g$. O$_2^-$ formation from aqueous HY–Na was shown directly by EPR [42,43]. The addition of 30 μg ml^{-1} SOD to HY–Na in PB/0.5%TX100 reduced Φ_c from 1.69 to 1.39, confirming that the LYS probe responds to O$_2^-$ [2]. The low values of the protection factors in the present work do not rule out small yields of O$_2^-$ in the presence of high $^1\Delta_g$. First consider a hypothetical case where only O$_2^-$ is generated, with $\beta_d = 1.00$, $\beta_o = 0.95$, and $\beta_p = 0.98$, leading to $p = 0.6$. However, if both $^1\Delta_g$ and O$_2^-$ are generated leading to $\beta_o = 0.70$ and $\beta_p = 0.73$, then p would be reduced to 0.1. The only direct measurement of the O$_2^-$ quantum yield for the present sensitizers we have found is for HP in TX100 which led to 0.07 at 355 nm based on the photo-oxidation of 1,4-benzoquinone [25].

4.3. Photodynamic efficiency

It may be desirable to perform a photodynamic irradiation at a specific wavelength in order to utilize a light source or minimize "inner filtering" by an endogenous absorber. The intrinsic efficiency of a photodynamic process can be quantified by a parameter (α) defined as the $^1\Delta_g$ generation rate (M s^{-1}) per unit incident power density (W cm^{-2}) at the irradiation wavelength λ (nm), per unit sensitizer concentration (M). An expression for α in terms of measurable quantities is

$$\alpha = 1.925 \times 10^{-5} \lambda \Phi_\Delta \epsilon_s \qquad (9)$$

where ϵ_s (M^{-1} cm^{-1}) is the sensitizer extinction coefficient. Table 6 summarizes approximate values of α calculated with the present data. The most efficient sensitizers in the far-red region are MB, PPIX, the chlorins, and AlPcS$_4$. HY is efficient at 590 nm. The values of α at 546 and 630 nm are comparable at the far-red peak for the porphyrins. Light penetration and the effects of competing absorbers must be considered for practical applications. The optimal irradiation wavelength involves a compromise between α and the effective attenuation coefficient (μ_{eff}) of the medium. Consider the photodynamic irradiation of whole blood. Some approximate values of $1/\mu_{eff}$ estimated from published optical constants [44,45] are 415 nm (0.002 mm), 545 nm (0.02 mm), 585 nm (0.72 mm), 633 nm (0.95 mm), 660 nm (2.7 mm), 800 nm (1.2 mm). Thus, blue and green light would be ineffective for any sensitizer, 585 nm and 633 nm would be about equally effective for thin layers, and wavelengths near 660 nm would be most effective for thick layers. Additional physiological factors are involved in vivo. In PDT, for example, the drug pharmacokinetics, sensitizer binding sites, and tissue oxygenation are other determinants of the tumor response. The α parameter may help delineate between the photophysical and physiological factors responsible for the observed wavelength effects. In a recent PDT study with BPD-MA in a mouse model, the tumor-free percentage of animals at 20 days-post PDT was about the same for 200 J cm^{-2} at 630 nm compared with 50 J cm^{-2} at 690 nm [46]. The light dose ratio for this endpoint is comparable with the ratio of the α values in Table 6. However, the same study reported that the photosensitivity of normal mouse skin was about the same at 630 and 690 nm for 125 J cm^{-2}. Physiological factors appear to dominate for this endpoint, possibly owing to the saturation of the skin damage at the high light dose.

4.4. Summary and conclusions

The LYS photosensitization technique used for measuring Φ_Δ of the photodynamic agents is fast and accurate. Consistent values were obtained for measurements at several different wavelengths. The present results are in good agreement with the published data based on other techniques. The concentration and wavelength effects on Φ_Δ for self-aggregating

Table 6
Photodynamic efficiency of sensitizers in TX100

Sens.	Φ_Δ [a]	$\alpha(cm^2 J^{-1})$ [b]		
		546 nm	630 nm	Far-red band
MB	0.49	30	100	668 nm: 490
HP	0.73	35	30	616 nm: 35
PPIX	0.56	140	110	646 nm: 125
ZnPP	0.91	60	70	606 nm: 75
TPPS	0.61	35	15	644 nm: 30
PF	0.89	55	30	623 nm: 50
Chl-e6 [c]	0.64	20	45	662 nm: 220
BPD-MA	0.84 [d]	60	80	687 nm: 320
Pheo-a	0.69	50	35	668 nm: 290
AlPcS$_4$	0.38	10	65	673 nm: 760
HY/HY-Na	0.49	105	-	597 nm: 230

[a] Average value from Table 1.
[b] $\alpha = 1.93 \times 10^{-5} \lambda$ (nm) $\Phi_\Delta \epsilon_s (M^{-1} cm^{-1})$.
[c] In PB.
[d] From Table 3.

HP and BPD-MA in PB are attributed to the monomer-dimer equilibria. Micellar interactions and binding to LYS for Chl-e6 led to negligible Φ_Δ in PB/TX100 and ineffective quenching by azide and DABCO in PB.

Acknowledgements

References

[1] L.R. Jones and L.I. Grossweiner, Singlet oxygen generation by Photofrin^R in homogeneous and light-scattering media, J. Photochem. Photobiol. B: Biol.; 26 (1994) 249-256.

[2] V. Senthil, L.R. Jones, K. Senthil and L.I. Grossweiner, Hypericin photosensitization in aqueous model systems, Photochem. Photobiol., 59 (1994) 40-47.

[3] V. Senthil, J.L. Longworth, C.A. Ghiron and L.I. Grossweiner, Photosensitization of aqueous model systems by hypericin, Biochim. Biophys. Acta, 1115 (1992) 192-199.

[4] N. Houba-Herin, C.M. Calberg-Bacq, J. Piette and A. Van der Vorst, Mechanisms of dye-mediated photodynamic action: Singlet oxygen production, deoxyguanosine oxidation and phage inactivating efficiencies, Photochem. Photobiol., 36 (1982) 297-306.

[5] A.G. Kepka and L.I. Grossweiner, Photodynamic inactivation of lysozyme by eosin, Photochem. Photobiol., 18 (1973) 49-61.

[6] H. Schmidt and P. Rosenkranz, On the mechanism of the acridine orange sensitized photodynamic inactivation of lysozyme, Z. Naturforsch., 31 (1976) 29-39.

[7] M.A.J. Rodgers and P.T. Snowden, Lifetime of $O^2(^1\Delta_g)$ in liquid water as determined by time-resolved infrared luminescence measurements, J. Am. Chem. Soc., 104 (1982) 5541-5543.

[8] Y. Usui and K. Kamogawa, A standard system to determine the quantum yield of singlet oxygen formation in aqueous solution, Photochem. Photobiol., 19 (1974) 245-247.

[9] D. Kessel, Interactions between N-apartyl chlorin e6, detergent micelles and plasma lipoproteins, Photochem. Photobiol., 61 (1995) 646-649.

[10] J.D. Spikes, Chlorins as photosensitizers in biology and medicine, J. Photochem. Photobiol. B: Biol., 6 (1990) 259-274.

[11] B.M. Aveline, T. Hasan and R.W. Redmond, The effects of aggregation, protein binding and cellular incorporation on the photophysical properties of benzoporphyrin derivative monoacid ring A (BPDMA), J. Photochem. Photobiol. B: Biol., 30 (1995) 161-169.

[12] G.R. Seely, Mechanisms of the photosensitized oxidation of tyramine, Photochem. Photobiol., 26 (1977) 115-123.

[13] J.R. Harbour and S.L. Issler, Involvement of the azide radical in the quenching of singlet oxygen by azide ion in water, J. Am. Chem. Soc., 104 (1982) 903-905.

[14] R.D. Hall and C.F. Chignell, Steady-state near-infrared detection of singlet molecular oxygen: a Stern-Volmer quenching experiment with sodium azide, Photochem. Photobiol., 45 (1987) 459-464.

[15] B.M. Monroe, Singlet oxygen in solution: lifetimes and reaction rate constants, in A.A. Frimer (ed.) Singlet O_2, Vol. I. CRC Press, Boca Raton, FL, 1985, pp. 177-224.

[16] F. Wilkinson and J.G. Brummer, Rate constants for the decay and reactions of the lowest electronically excited singlet state of molecular oxygen in solution, J. Phys. Chem. Ref. Data, 10 (1981) 809-999.

[17] J.D. Spikes and J.C. Bommer, Photosensitizing properties of mono-L-aspartyl chlorin e$_6$ (NPe6): a candidate for the photodynamic therapy of tumors, J. Photochem. Photobiol. B: Biol., 17 (1993) 135-143.

[18] T.R. Hopkins and J.D. Spikes, Conformational changes in lysozyme during photodynamic inactivation, Photochem. Photobiol., 12 (1970) 175-184.

[19] H. Schmidt, A. Al-Ibrahim, U. Dietzel and L. Bieker, On the acridine orange and thiazine dye sensitized photodynamic inactivation of lysozyme-singlet oxygen self-quenching by the sensitizers, Photochem. Photobiol., 33 (1981) 127-130.

[20] W. Poppe and L.I. Grossweiner, Photodynamic sensitization by 8-methosypsoralen via the singlet oxygen mechanism, Photochem. Photobiol., 22 (1975) 217-219.

[21] J.N. Chacon, J. McLearie and R.S. Sinclair, Singlet oxygen yields and radical contribution in the dye-sensitized photo-oxidation in methanol esters of polyunsaturated fatty acids (oleic, linoleic, linolenic and arachidonic), Photochem. Photobiol., 47 (1988) 647-656.

[22] E. Gross, B. Ehrenberg and F.M. Johnson (1993) Singlet oxygen generation by prophyrins and the kinetics of 9,10-dimethylanthracene photosensitization in liposomes., *Photochem. Photobiol., 57* (1993) 808-813.

[23] A. Blum and L.I. Grossweiner, Singlet oxygen generation by hematoporphyrin IX, Uroporphyrin I and hematoporphyrin derivative at 546 nm in phosphate buffer and in the presence of egg phosphatidylcholine liposomes, *Photochem. Photobiol., 41* (1985) 27-32.

[24] C. Tanielian and C. Wolff, Determination of the parameters controlling singlet oxygen production via oxygen heavy-atom enhancement of triplet yields, *J. Phys. Chem., 99* (1995) 9831-9837.

[25] E. Reddi, G. Jori, M.A. J. Rodgers and J.D. Spikes, Flash photolysis studies of hemato- and copro-porphyrins in homogeneous and microheterogeneous aqueous dispersions, *Photochem. Photobiol., 38* (1983) 639-645.

[26] C. Tanielian and G. Heinrich, Effect of aggregation on the hematoporphyrin-sensitized production of singlet molecular oxygen, *Photochem. Photobiol., 61* (1995) 131-133.

[27] J.D. Spikes, Quantum yields and kinetics of the photobleaching of hematoporphyrin, Photofrin II, tetra(4-sulfonatophenyl)porphine and uroporphyrin, *Photochem. Photobiol., 55* (1992) 797-808.

[28] J.P. Keene, D. Kessel, E.J. Land, R.W. Redmond and T.G. Truscott, Direct determination of singlet oxygen sensitized by hematoporphyrin and related compounds, *Photochem. Photobiol., 43* (1986) 117-120.

[29] J. Feitelson and N. Barboy, Triplet-state reactions of zinc protoporphyrins, *J. Am. Chem. Soc., 90* (1986) 271-274.

[30] M.A.J. Rodgers, Singlet oxygen quantum yields, in J.R. Heitz and K.R. Downum (eds.), *Light-Activated Pesticides*, ACS Symposium Series 339., Washington, D.C., 1987, pp. 76-97.

[31] J.B. Verlhac, A. Gaudemer and I. Kraljic, Water-soluble porphyrins and metalloporphyrins as photosensitizers in aerated aqueous solutions. I. Detection and determination of quantum yield of formation of singlet oxygen, *Nouv. J. Chim., 8* (1984) 401-406.

[32] S. Kimel, B.J. Tromberg, W.G. Roberts and M.W. Berns, Singlet oxygen generation of porphyrins, chlorins and phthalocyanines, *Photochem. Photobiol., 50* (1989) 175-183.

[33] K. Konig, H. Schneckenburger, A. Ruck and R. Steiner, *In vivo* photoproduct formation during PDT with ALA-induced endogenous porphyrins, *J. Photochem. Photobiol. B:Biol., 18* (1993) 287-290.

[34] I.M. Vyteva, M.V. Sarzhevskaya, G.A. Kochubeev and P.P. Guronovich, Photochemical reaction of chlorin e_6 with oxygen in aqueous media, *J. Appl. Spectrosc., 46* (1987) 626-629.

[35] B. Aveline, T. Hasan and R.W. Redmond, Photophysical and photosensitizing properties of benzoporphyrin derivative monoacid ring A (BPD-MA), *Photochem. Photobiol., 59* (1994) 328-335.

[36] A.A. Karasnovsky, Jr., K.V. Neverov, S. Yu. Egorov, B. Roeder and T. Levald, Photophysical studies of pheophorbide *a* and pheophytin *a* phosphorescence and photosensitized singlet oxygen luminescence, *J. Photochem. Photobiol., B. Biol., 5* (1990) 248-254.

[37] A. Telfer, S.M. Bishop, D. Phillips, and J. Barber, Isolated photosynthetic reaction center of photosystem II as a sensitizer for the formation of singlet oxygen, *J. Biol. Chem., 269* (1994) 13244-13253.

[38] J. Davila and A. Harriman, Photosensitized oxidation of biomaterials and related model compounds, *Photochem. Photobiol., 50* (1989) 29-35.

[39] I. Rosenthal, C. Murali Krishna, P. Riesz and E. Ben-Hur, The role of molecular oxygen in the photodynamic effect of phthalocyanines, *Radiat. Res., 107* (1986) 136-142.

[40] H. Racinet, P. Jardon and R. Gautron, Formation d'oxygène singulet $^1\Delta_g$ photosensibilise par l'hypericine. Tube cintique en milieu micellaire non ionique, *J. Chim. Phys., 85* (1988) 971-977.

[41] L.I. Grossweiner and A.G. Kepka, Photosensitization in biopolymers, *Photochem. Photobiol., 16* (1972) 305-314.

[42] L. Weiner and Y. Mazur, EPR studies of hypericin. Photogeneration of free radicals and superoxide, *J. Chem. Soc. Perkin Trans., 2* (1992) 1439-1442.

[43] Z. Diwu and J.W. Lown, Photosensitization with anticancer agents, 17. EPR studies of photodynamic action of hypericin: formation of semiquinone radical and activated oxygen species on illumination, *Free Radic. Biol. Med., 14* (1993) 209-215.

[44] M.J.C. van Gemert, A.J. Welch, I.D. Miller, and O.T. Tan, Can physical modeling lead to an optimal laser treatment for port-wine stains? in M.L. Wolbarsht (ed.) *Laser Applications in Medicine and Biology*, Vol. 5, Plenum Press, New York, 1991, p. 199-275.

[45] J.M. Steinke and A.P. Shepherd, Diffusion model of the optical absorbance of whole blood, *J. Opt. Soc. Am. A, 5* (1988) 813-822.

[46] E.M. Waterfield, M.E. Renke, C.B. Smits, M.D. Gervais, R.D. Bower, M.S. Stonefield and J.G. Levy, Wavelength-dependent effects of benzoporphyrin derivative monoacid ring A *in vivo* and *in vitro*, *Photochem. Photobiol., 60* (1994) 383-387.